

Cu(II) Adsorption on Modified Bentonitic Clays: Different Isotherm Behaviors in Static and Dynamic Systems

Ambrósio Florêncio de Almeida Neto^{a*}, Melissa Gurgel Adeodato Vieira^b,

Meuris Gurgel Carlos da Silva^a

^aDepartment of Thermo-fluidynamics, School of Chemical Engineering,
State University of Campinas – UNICAMP, Av. Albert Einstein, 500,
Cidade Universitária “Zeferino Vaz”, CEP 13083-852, Campinas, SP, Brazil

^bDepartment of Chemical Processes, State University of Campinas – UNICAMP,
Av. Albert Einstein, 500, Cidade Universitária “Zeferino Vaz”,
CEP 13083-852, Campinas, SP, Brazil

Received: July 26, 2011; Revised: September 16, 2011

Cu (II) removal equilibrium from aqueous solutions using calcined clays “Bofe” and “Verde-lodo” has been studied by batch and fixed-bed in static and dynamic systems, respectively. Analyses were performed for physicochemical characterization of clays using the techniques: X-ray fluorescence (XRF), thermogravimetry (TG), N₂ adsorption (BET) and Cationic Exchange Capacity (CEC). Batch experiments were performed at a constant temperature, adjusting the pH of the solution in contact with clays. Adsorption assays in fixed bed were conducted at the flow rate determined through mass transfer zone (MTZ). Langmuir and Freundlich models were adjusted to equilibrium data. The results of characterization indicated that the temperature of 500 °C is best suited for the calcination of the clays. The maximum adsorption capacity was higher for dynamic system than fixed bed compared to static system, enhancing from 0.0748 to 0.1371 and from 0.0599 to 0.22 mmol.g⁻¹ of clay for “Bofe” and “Verde-lodo”, respectively.

Keywords: adsorption, heavy metal removal, bentonitic clay

1. Introduction

Clays and minerals such as montmorillonite, vermiculite, illite, kaolinite and bentonite are known as alternative materials used to adsorption of heavy metal due to several economic advantages¹⁻⁹ and their intrinsic properties, such as large specific surface area, excellent physical and chemical stability and properties structural and surface¹⁰. Other low-cost adsorbents have been investigated, mainly using bioadsorbents, such as algae¹¹ and chitosan¹². However, experiments carried out in fixed bed presented limited results. Bentonite clays are widely used as barriers to avoid subsoil and underground landfill water contamination by leaching containing heavy metals.

Although the results obtained in metal removal using clays are significant and promising, a better understanding of these results is still needed. Studies already performed on Brazilian calcined clay (Bofe type) in the removal of nickel^{13,14} have shown the need for further research on heavy metal removal comparing adsorption capacity in both static and dynamic systems. The high load of galvanic toxic waste in the Southeast of Brazil is composed mainly of salts of cyanide and heavy metals such as copper, among others; these can be present in soluble and insoluble forms. Therefore, research on the mechanisms of removal of copper are required for remediation of this contaminant.

In order to evaluate the removal of copper using Bofe and Verde-Lodo (VL) bentonite clays as adsorbents thermally modified, the adsorption experiments were conducted using static (batch) and dynamic systems (fixed-bed). Both clays have been chosen due to their relevant adsorptive properties¹³ and abundance in the Brazil. Modified clays have shown enhanced adsorption capacity.

2. Experimental

2.1. Adsorbents

Two types of bentonite clays “Bofe” and “Verde-lodo (VL)” from the Northeastern region of Brazil (Boa Vista-PB) were used as adsorbents. Initially, a study was conducted with both raw clays. However, these clays were not used in fixed bed as adsorbents due to their solubility. The clays were prepared by size classification and calcined at 500 °C for 24 hours in order to increase their mechanical resistance, dehydroxylation and to eliminate some impurities. In some cases, the adsorption capacity can also be enhanced on modified bentonitic clays. The temperature of calcination was determined by thermogravimetric analysis for samples Bofe and VL clays at a heating rate of 10 °C/min in air atmosphere.

*e-mail: ambrosio@feq.unicamp.br

2.2. Metal adsorbate

The adsorption tests were performed using an aqueous solution in $15.74 \text{ mmol.L}^{-1}$ of copper metal, prepared dissolving appropriate amount of $\text{Cu}(\text{NO}_3)_2 \cdot 3\text{H}_2\text{O}$ in deionized water to desired concentrations.

The Cu(II) solution pH was maintained at a level lower, minimizing the precipitation in to assure the occurrence of the adsorption process and avoiding the chemical precipitation of copper ions in the hydroxide form ($\text{Cu}(\text{OH})_2$). The pH of the solutions was measured with pH-meters and it was kept at set values using nitric acid and ammonium hydroxide.

2.3. Metal speciation

Copper speciation diagrams were simulated using Hydra and Medusa softwares¹⁵ to identify the different species in solution. Speciation was investigated considering the used stoichiometric ratio of copper salt.

2.4. Clay characterization

The chemical composition of raw and calcined samples of Bofe and VL clays were obtained by X-ray fluorescence analysis, using samples fused in borate matrix.

Thermogravimetric analysis was carried out on a Micromeritics TGA in N_2 atmosphere (50 mL/min) at a heating rate of $10 \text{ }^\circ\text{C/min}$. The samples were putted in platinum pans and scanned from room temperature to $1000 \text{ }^\circ\text{C}$.

The surface area was obtained by N_2 physisorption at 77 K using the BET method.

The Cation Exchange Capacity (CEC) was determined in triplicate for raw and calcined samples of Bofe and VL clays. The ions concentration of Na^+ displaced by the NH_4OH exchange solutions were measured by Atomic Absorption and expressed in $\text{meq} (100 \text{ g})^{-1}$ of solid according to Equation 1:

$$\text{CEC} = \frac{C_{\text{Na}^+} \cdot V_{\text{NH}_4^+}}{10 \cdot m \cdot f} \quad (1)$$

The zero-point load of solid elements in suspension (pH_{zpc}) was obtained using the potentiometrical titration methodology¹⁶. The titration was carried out with 0.5 M CH_3COOH and 0.5 M NH_4OH . For each point of the titration, was obtained by Equation 2:

$$S = \frac{C_a - C_b + [\text{OH}^-] - [\text{H}^+]}{A \cdot C_m} \cdot F \quad (2)$$

For CH_3COOH or NH_4OH addition, S can be expressed as either by Equations 3 and 4:

$$S = \frac{C_a - [\text{H}^+]}{A \cdot C_m} \cdot F \quad (3)$$

$$S = \frac{[\text{OH}^-] - C_b}{A \cdot C_m} \cdot F \quad (4)$$

2.5. Batch sorption procedure

The adsorption experiments were performed using an aqueous solution of $\text{Cu}(\text{NO}_3)_2 \cdot 3\text{H}_2\text{O}$ in fixed concentrations, with temperature controlled under constant stirring of 150 rpm . At specific time intervals, solution aliquots were removed and centrifuged. The supernatant liquid was diluted and its concentration was determined by atomic absorption spectrometry.

To evaluate the effect of contact time, the experiments were conducted using 1 g of clay per 100 mL of copper solution at 1.57 mmol.L^{-1} concentration. Temperature and pH were kept at 298 K and 5.0 , respectively. The samples were shaken for 300 minutes .

Equilibrium tests were performed with different concentrations of adsorbate and temperatures. For maintaining pH of the medium, solutions of 0.01 M HNO_3 or 0.01 M $\text{NH}_4(\text{OH})$ were added to adjust the pH value. The pH was monitored before and after adsorption. The following conditions were maintained for the different sets of experiments:

i) Effects of adsorbate concentration and adsorption isotherm: clay $1 \text{ g}/100 \text{ mL}$.

ii) Thermodynamics: clay $1 \text{ g}/100 \text{ mL}$, time 300 minutes , pH 5.0 , temperature $273, 298, 323$ and 348 K .

Langmuir's theoretical model¹⁷ (Equation 5) and Freundlich's empirical model¹⁸ (Equation 6) were adjusted to the adsorption isotherms.

$$q_{\text{eq}} = \frac{q_m \cdot b \cdot C_{\text{eq}}}{1 + b \cdot C_{\text{eq}}} \quad (5)$$

$$q_{\text{eq}} = (K_f \cdot C_{\text{eq}})^n \quad (6)$$

The adsorbed amount was obtained by Equation 7:

$$q = \frac{V(C_i - C_f)}{m} \quad (7)$$

The essential characteristics of the Langmuir isotherm can be expressed by the separation factor or equilibrium parameter (RL) given by Equation 8:

$$R_L = \frac{1}{1 + b \cdot C_0} \quad (8)$$

The parameter RL indicates the curvature of the sorption isotherm: if $RL > 1$, the isotherm is not favorable; if $RL = 1$, linear behavior; $0 < RL < 1$, favorable; $RL = 0$, irreversible.

The thermodynamic parameters for the adsorption process ΔH (kJ.mol^{-1}), ΔS ($\text{J}(\text{K.mol}^{-1})$) and ΔG (kJ.mol^{-1}) were evaluated using thermodynamic Equations 9 and 10:

$$\Delta G = -RT \ln(K_d) \quad (9)$$

$$\ln(K_d) = -\frac{\Delta G}{RT} = \frac{\Delta S}{R} - \frac{\Delta H}{RT} \quad (10)$$

The $\ln(K_d)$ vs. $1/T$ graph must be linear with inclination of the straight line ($-\Delta H/R$) and intercept the y axis at ($\Delta S/R$), providing the values for ΔH and ΔS . The variation in Gibbs free energy (ΔG) is the fundamental criterion of the process spontaneity.

Table 1. Chemical clay for Bofe and VL analyses.

| Sample | Composition (%) | | | | | | | | | | | |
|---------------|-----------------|------------------|--------------------------------|------------------|--------------------------------|------|------|-------------------|------------------|------|-------------------------------|--------|
| | LOI* | SiO ₂ | Al ₂ O ₃ | TiO ₂ | Fe ₂ O ₃ | CaO | MgO | Na ₂ O | K ₂ O | MnO | P ₂ O ₅ | Total |
| Raw bofe | 7.09 | 70.10 | 13.64 | 0.63 | 5.44 | 0.31 | 2.08 | 0.58 | 0.16 | 0.01 | 0.03 | 100.06 |
| Calcined bofe | 3.77 | 69.03 | 14.28 | 0.57 | 6.94 | 0.46 | 4.50 | 0.24 | 0.15 | 0.01 | 0.04 | 100.00 |
| Raw VL | 8.72 | 54.29 | 19.71 | 1.30 | 9.27 | 0.76 | 3.30 | 0.64 | 1.94 | 0.03 | 0.06 | 100.01 |
| Calcined VL | 4.38 | 54.13 | 19.36 | 0.93 | 15.14 | 0.48 | 4.13 | 0.27 | 1.08 | 0.05 | 0.05 | 99.99 |

*Loss on ignition.

2.6. Column sorption procedure

Adsorption experiments were performed in a porous bed system, consisting of an acrylic column, with 14 cm of height and 1.4 cm of internal diameter. The operating conditions were based on the experimental design, considering the study conducted in batch and preliminary fixed-bed tests.

In order to determine the mass transfer zone, the amount of useful and total removal were calculated, which correspond to the capacity of metal removal until the breakthrough point (q_U) and saturation point (q_T), respectively. Equations 11 and 12 were obtained through the mass balance in the column using saturation data, based on its breakthrough curves, where the area below the curve ($1-C/C_0$) until the breakthrough point is proportional to q_U , and area until the bed exhaustion is proportional to q_T :

$$q_U = \frac{C_0 \cdot Q}{1000 \cdot m} \int_0^{t_b} \left(1 - \frac{C|_{z=L}}{C_0}\right) dt \quad (11)$$

$$q_T = \frac{C_0 \cdot Q}{1000 \cdot m} \int_0^{t_{tot}} \left(1 - \frac{C|_{z=L}}{C_0}\right) dt \quad (12)$$

MTZ can then be calculated based on the q_U/q_T ratio according to Equation 13.

$$MTZ = H_L \cdot \left(1 - \frac{q_U}{q_T}\right) \quad (13)$$

MTZ has a maximum value which corresponds to the bed height (H_L) and when the efficacy of mass transference increases. This value decreases until reaching the ideal condition, where MTZ is zero and the breakthrough curve is a step function.

The percentage of total removal (%RT) during adsorption was obtained considering the metal fraction in solution retained in the adsorbent solid, from total effluent used in the adsorption process until bed saturation. The amount of adsorbed metal is calculated by considering the area of the curve ($1-C/C_0$) vs. t^{19} using Origin version 6.0 software.

3. Results and Discussion

3.1. Bofe and VL clays characterization

The chemical composition of the compounds raw and calcined of the Bofe and VL clays obtained by XRF are shown in Table 1. The average composition is consistent with the expected for this bentonite clay²⁰. One can observe

Table 2. Cationic clay exchange capacity (CEC) and surface area.

| Sample | CEC (meq (100 g) ⁻¹) | Surface area (m ² .g ⁻¹) |
|---------------------|----------------------------------|---|
| Raw Bofe | 93.33 ± 5.74 | 78.61 ± 1.14 |
| Calcined Bofe | 55.65 ± 4.26 | 90.31 ± 3.65 |
| Raw Verde-lodo | 87.54 ± 2.46 | 64.31 ± 3.13 |
| Calcined Verde-lodo | 47.83 ± 2.46 | 62.08 ± 0.52 |

that the Bofe and VL clays are a polycationic bentonite due to the presence of Ca²⁺, Mg²⁺ and Na⁺ cations in both raw and calcined clay samples.

Cationic capacity result exchanges (CEC) of raw and calcined clays and superficial respective areas obtained by BET are shown in the Table 2.

Smectite clays from Paraíba generally present CEC values between 50 e 90 meq (100 g)⁻¹ of clay²⁰. Relatively high CEC values of raw clays indicated that they have a high isomorphous replacement level. On the other hand, calcined smectites at 500 °C have their exchange cation capacity drastically reduced in comparison to raw CEC clays. The high value of CEC with respect to the raw clays indicates that the minerals have a high level of isomorphous substitutions. In addition, the smectite calcined at 500 °C has a lower ability to exchange cations in relation to the raw clay.

The values obtained to surface area by the BET method for raw and calcined Bofe clays were of 78.61 and 90.31 m².g⁻¹, respectively, whereas for samples of VL clays the values were of 64.31 and 62.08 m².g⁻¹, in the same order.

Figure 1 shows TG and DTG curves for raw Bofe and VL clays. The DTG curve presents two peaks of mass loss. The first, between 50-105 °C refers to the loss of water, volatile compounds, microorganisms and organic material; these elements do not change clay structure. Mass losses occurred for two temperatures and correspond to 4.82 and 3.57% of mass. The second peak occurring between 450-500 °C shows the loss of hydroxyl, which starts to change the clay structure. Hydroxyl loss is interesting for the process, because it prevents the chemical precipitation of copper by alkalinity and it increases the clay stability for its application in fixed-bed adsorption columns.

According to Figure 2, the pH_{ZPC} values obtained for raw and calcined clays were of 6.1 and 5.4, respectively. Thus, in order to ensure that the calcined clay surface has a null or negative charge with the aim of making more favorable the adsorption of charged positively metal ions, the adsorbate solution pH should be kept in 5.5.

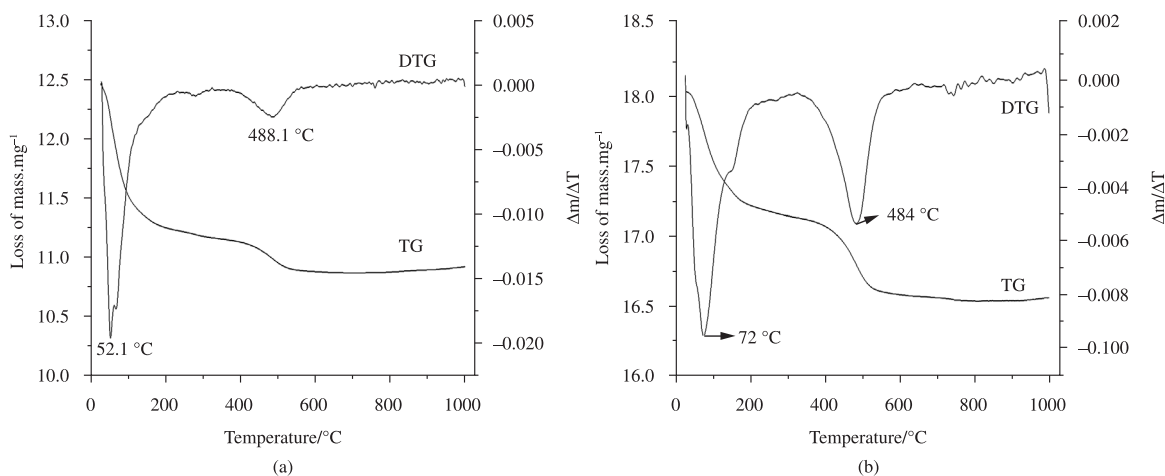


Figure 1. TG and DTG curves of raw: a) Bofe; and b) VL clays.

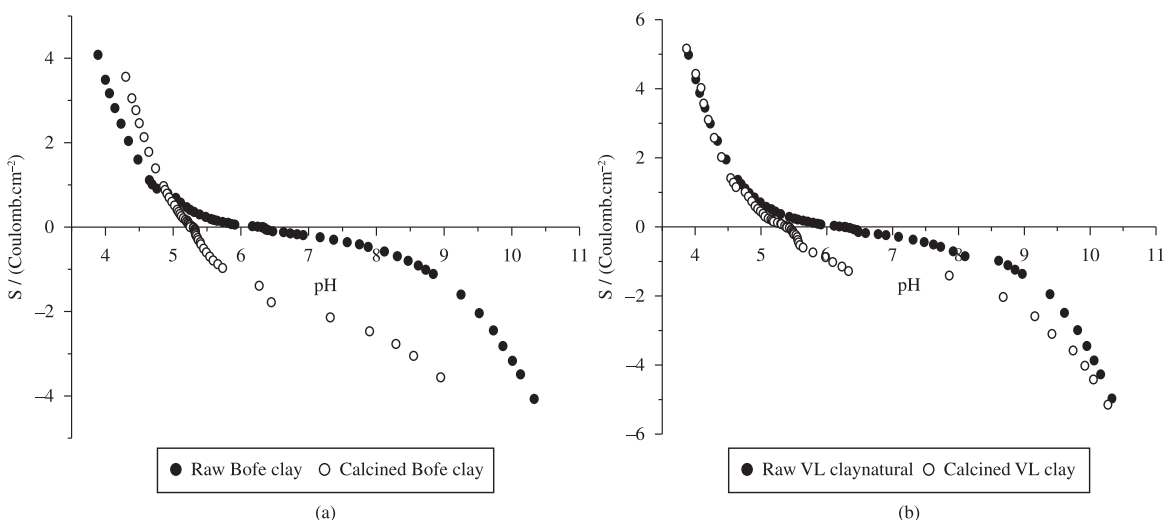


Figure 2. Charge density (Coulomb cm^{-2}) vs. pH curves of: a) Bofe, and b) VL clay samples.

3.2. Copper speciation

The Figure 3 shows the speciation curve of the Cu^{2+} ion in aqueous solution with nitrate ions at different concentrations determined through the HYDRA application. In the pH range of 4.8-5.3, the fraction of Cu^{2+} ions in aqueous solution decreases and beginning the formation of copper oxide, which is precipitates. With the purpose that only the adsorption occurs, should be used a pH value below minimum precipitation, which corresponds to 5.0 for concentration of 1.57 mmol.L^{-1} .

3.3. Batch adsorption

Figure 4a and b present the curve for copper adsorption kinetics on Bofe and VL clays. The adsorption of copper ions into pores of clays occurred rapidly at the first moments of the process, remaining at equilibrium over time. The reduction of the initial concentration of the ion, under the condition of this study, was around 81% in both raw clays and around 42% in both calcined clays. The maximum

adsorbed amount was around 0.13 and 0.08 mmol of copper g^{-1} of clay for raw and calcined clays, respectively.

Through kinetic studies at static system, it is verified that removal capacity is reduced by clay calcinations. However, in preliminary tests, raw clays could not be applied in fixed bed due to their mechanical instability. When the raw clays were in contact with copper salt solutions, the clay adsorbed a great quantity of water, expanding the volume bed due to their blade defoliation, which are dissolved and dispersed along the flow, being the clay dragged down through the column when the flow is ascendant. At a descendent flow use, a bed waterproofing was also observed.

On the other hand, clays also get steel hardness at temperatures above $180 \text{ }^{\circ}\text{C}$ ²⁰. This fact, associated with Bofe¹³ and VL clay characterization results, suggest that the calcination provides to the materials mechanical stabilization (not dissolving), getting that these do not expand or being waterproof in porous column. Therefore, the calcined Bofe and VL clays are more appropriated to be used as adsorbent for copper removal in fixed bed.

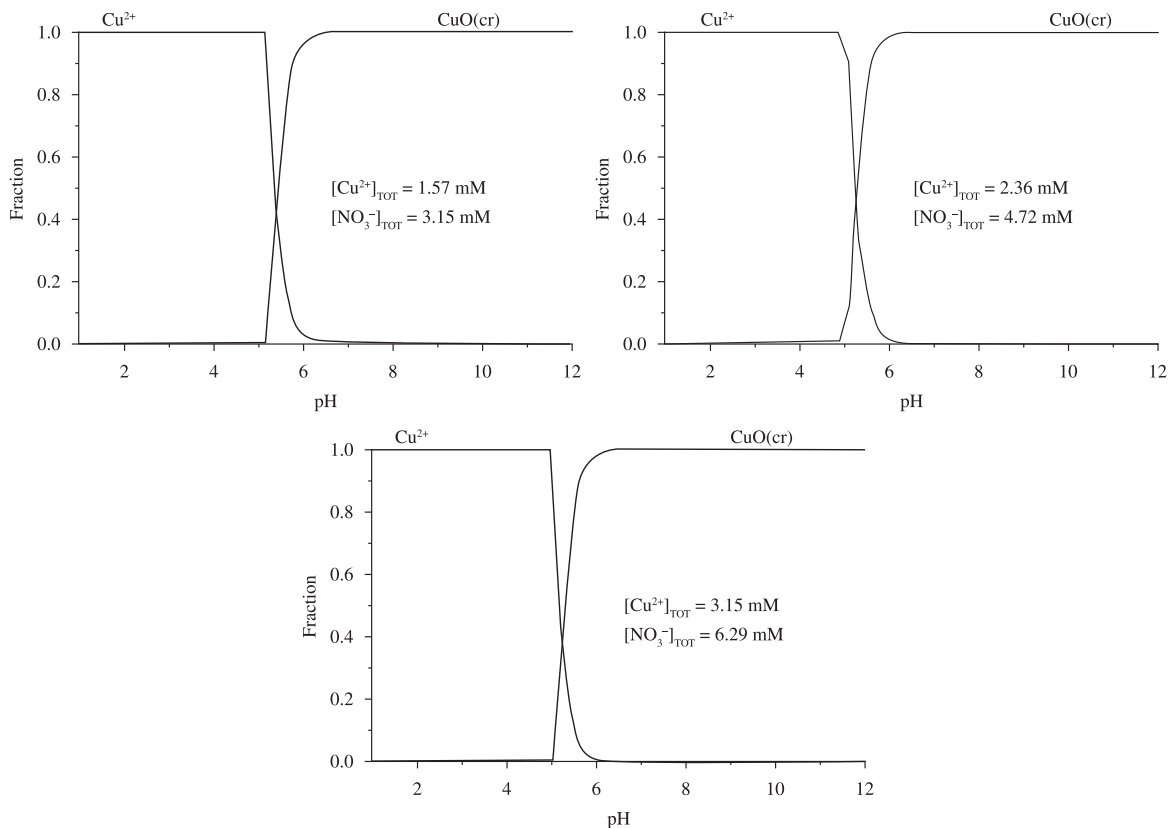


Figure 3. Copper speciation.

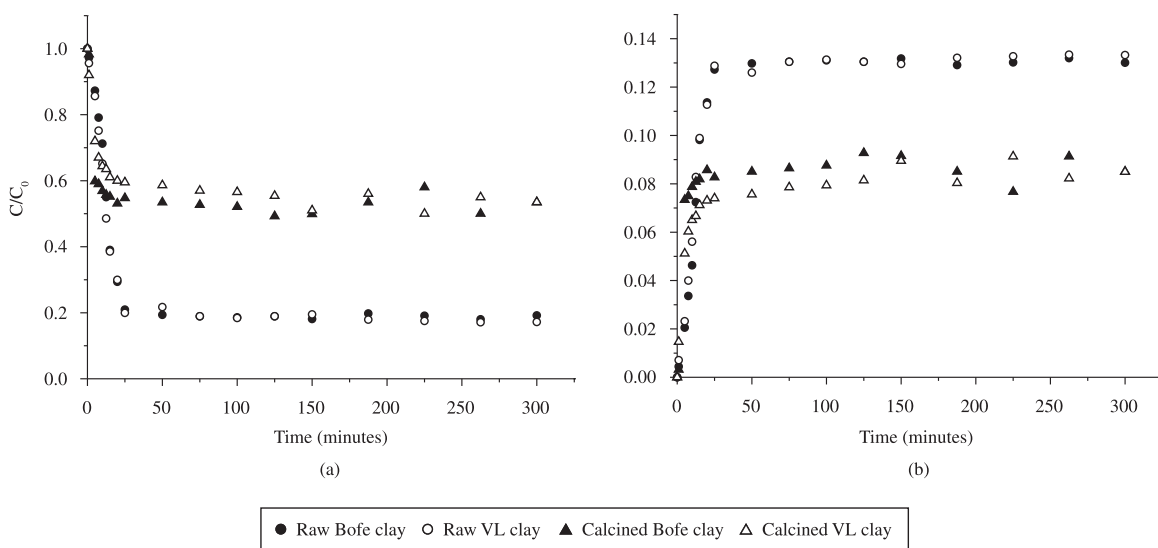


Figure 4. Kinetic for copper adsorption on clays. a) Dimensionless solution concentration as a function of time, and b) Adsorbed amount at equilibrium ($C_0 = 1.57 \text{ mmol L}^{-1}$, $d_p = 0.855 \text{ mm}$).

3.4. Dynamic adsorption

Dynamic adsorption experiments were carried out for different flow rates, varying values from 2.0 to 6.0 mL/min for Bofe and from 2.0 to 5.0 mL/min for VL clay (Figure 5). The definition of appropriate flow rate was based on mass

transfer zone determination. The concentration values of copper adsorbate solution were 2.36 and 1.57 mmol.L^{-1} for adsorption on Bofe and VL clays, respectively. The breakthrough curves present distinct behaviors indicating the flow influence on diffusional resistances. The adsorption process presents strong resistance to bed saturation for the

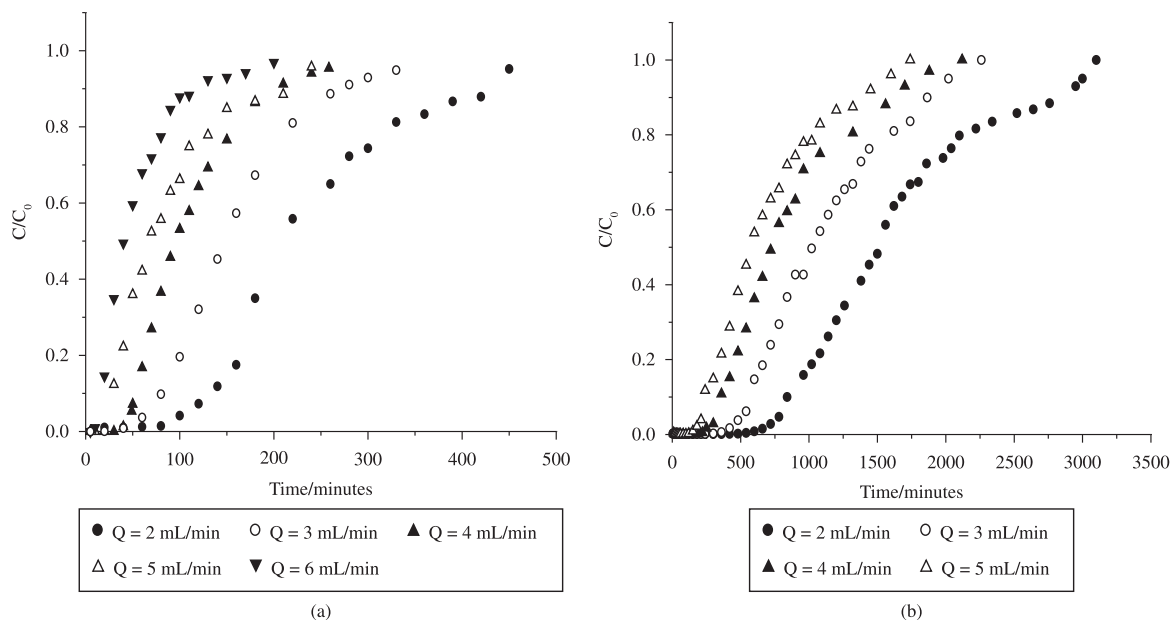


Figure 5. Breakthrough curves for: a) Cu^{2+} /Bofe calcined clay ($C_0 = 2.36 \text{ mmol.L}^{-1}$, $d_p = 0.855 \text{ mm}$), and b) Cu^{2+} /VL calcined clay ($C_0 = 1.57 \text{ mmol.L}^{-1}$, $d_p = 0.855 \text{ mm}$).

total flow range studied, it was known by the more extended breakthrough curves and broader mass transfer zones.

Table 3 shows the values of MTZ , qU , qT and copper removal percentage on calcined clays. The least MTZ value (7.77 cm), as well as satisfactory values of amount of useful (qU) and total removal (qT) and total removal percentage was obtained at 4.0 mL/min for copper adsorption on calcined Bofe clay. For copper adsorption on calcined VL clay, the least MTZ value (7.35 cm) was obtained at 2.0 mL/min, but the breakthrough curve showed high resistance of saturation. Then, the most appropriate flow value for conducting the copper adsorption on calcined VL clay assays was 3.0 mL/min.

The reproducibility of adsorption experiments can be seen in Figure 6, which shows breakthrough curves resulting from three performed tests at 4.0 and 3.0 mL/min for copper removal on calcined Bofe and VL clays, respectively. These results confirm the good reproducibility of the experimental, with a 0.34 and 0.33% average deviation for copper adsorption on calcined clays Bofe and VL, respectively. The variation curves are basically due to the axial bed dispersion and this phenomenon was not considered in the study.

3.5. Adsorption isotherms

The amount adsorbed of metal ions per mass unit of clay (q_{eq}) gradually increases as the initial concentration of the adsorbate solution increases, in both systems (batch and fixed bed). When the initial solution has a low concentration, the ratio between the number of ions and the number of adsorptive sites available is small; consequently, adsorption depends on the initial concentration. Therefore, as the concentration of ions increases, adsorption also increases. In high concentrations of ion, each unit mass of adsorbent is subjected to a larger number of ions, which depending on

Table 3. Values for MTZ , qU , qT and %RT for copper adsorption on calcined Bofe and VL clays.

| System | Outflow (mL/min) | MTZ (cm) | qU (mmol.g ⁻¹) | qT (mmol.g ⁻¹) | %RT |
|-----------------------|------------------|------------|------------------------------|------------------------------|-------|
| Cu/calcined Bofe clay | 2 | 7.81 | 0.0422 | 0.1056 | 52.10 |
| | 3 | 8.1 | 0.0417 | 0.1106 | 34.71 |
| | 4 | 7.77 | 0.0396 | 0.0985 | 41.86 |
| | 5 | 10.04 | 0.0228 | 0.1006 | 35.48 |
| | 6 | 10.98 | 0.0114 | 0.0732 | 25.83 |
| Cu/calcined VL clay | 2 | 7.35 | 0.0784 | 0.1648 | 49.82 |
| | 3 | 7.66 | 0.0796 | 0.1761 | 55.26 |
| | 4 | 8.81 | 0.067 | 0.1808 | 40.02 |
| | 5 | 9.98 | 0.048 | 0.167 | 49.70 |

the system can present different behaviors, as can be seen in Figure 7. The Langmuir and Freundlich models were adjusted to experimental data through the Gauss-Newton nonlinear estimation method in the Statistic 7.0 for Windows® software. The regression coefficients for both adjustments are shown in Table 4. The obtained parameters expressed by Equations 6 and 7 were associated with the process temperature.

Analyzing Figure 7 and Table 4, it can be seen that Langmuir model simulated adequately the experimental adsorption isotherm data for Bofe clay in batch and for VL clay in fixed bed system, while Freundlich empiric model described more efficiently the adsorption isotherm data for Bofe clay in fixed bed and for VL clay in batch system.

From the adsorption isotherms data, the maximum adsorbed capacities obtained in fixed bed system for both clays is higher than the results got in batch, which means that copper adsorption on Bofe and VL clays is related to

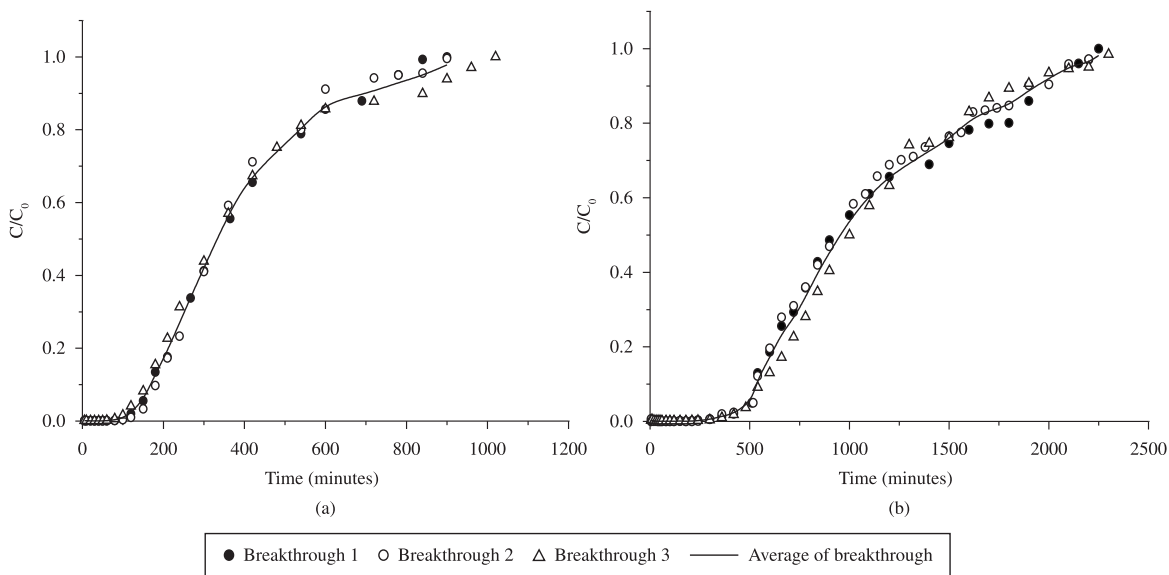


Figure 6. Reproducibility of breakthrough curves for copper adsorption on calcined clays: a) Bofe, and b) VL ($C_0 = 1.57 \text{ mmol.L}^{-1}$, $d_p = 0.855 \text{ mm}$).

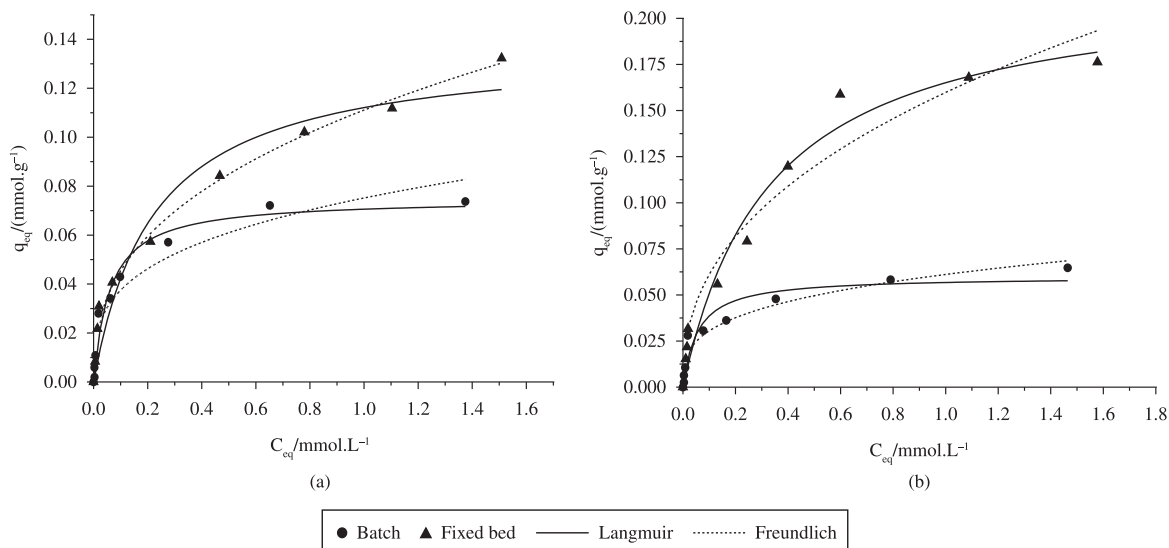


Figure 7. Adsorption isotherms for copper removal on: a) calcined Bofe clay, and b) calcined VL clay, adjusted to the models Langmuir and Freundlich.

Table 4. Langmuir and Freundlich parameters for Cu^{2+} adsorption on Bofe and VL clays.

| System | Langmuir | | | Freundlich | | |
|---------------------------|-----------------------------------|-------------------------------|--------|------------|--------|--------|
| | $qm \text{ (mmol.g}^{-1}\text{)}$ | $b \text{ (L.g}^{-1}\text{)}$ | R^2 | a | n | R^2 |
| Cu/calcined Bofe/batch | 0.0748 | 16.7868 | 0.9725 | 0.0752 | 0.3015 | 0.9259 |
| Cu/calcined Bofe/fixe bed | 0.1371 | 4.4815 | 0.9478 | 0.1111 | 0.3877 | 0.922 |
| Cu/calcined VL/batch | 0.0599 | 18.198 | 0.9288 | 0.0611 | 0.3009 | 0.9378 |
| Cu/calcined VL/fixe bed | 0.22 | 3.0089 | 0.9718 | 0.1598 | 0.4175 | 0.951 |

the mobility of the particles. This behavior indicates that at higher concentrations of metal solution in batch occurred a formation of the electrical double layer, i. e., ions of the Stern layer and part of the diffuse layer. They form an ionic cloud around the particle, being attracted by the electric potential, which moves along with it during the flow of the suspension²¹. As a result, the particles start to behave as flow units of higher dimensions, whose radius is defined as the hydrodynamic radius of the particle, which decreases the maximum adsorbed capacity of copper on calcined clays. However, this behavior is not observed in Henry's infinite dilution region, that is, at very low concentrations.

The Langmuir isotherm is specific for monolayer adsorption, which was the case in this study, while the Freundlich model is better applied to adsorption at heterogeneous sites on the surface of a solid, with a mechanism that has not yet been established. The Langmuir equilibrium coefficient b determines the direction to which the equilibrium adsorbate-adsorbent clay (solid phase) + Cu(II) (aqueous phase) = clay-Cu(II) moves. Higher values indicate that the equilibrium moves to the right side, with the resulting formation of the adsorbate-adsorbent complex.

The values obtained for the Freundlich constant (n) are around 0.3 and 0.4 for adsorption in batch and in fixed bed, respectively. According to Treybal,²² this range indicates that the adsorptive characteristics of the clay are suitable for copper sorption.

The values calculated for RL (Equation 8) determined by using the Langmuir constant obtained by the nonlinear

method vs. the initial copper concentration for different systems were of 0.3076 (Cu/calcined Bofe/Batch), 0.6995 (Cu/calcined Bofe/fixed bed), 0.2907 (Cu/calcined VL/Batch) and 0.7682 (Cu/calcined VL/fixed bed). According to the separation values, both adsorption systems can be considered favorable to copper sorption ($0 < RL < 1$), being more favorable to sorption conducted in batch.

3.6. Adsorption thermodynamics

Thermodynamic data were obtained through the static method in thermostatic finite bath under constant stirring for four different temperatures (273, 298, 323 and 348 K) and correlated by the Langmuir and Freundlich isotherms. The Figure 8 shows the adsorption isotherms for 1 g clay/100 mL adsorbate solution adjusted by the Langmuir and Freundlich models, at initial copper concentrations ranging from 0.08 to 2.36 mmol.L⁻¹.

The thermodynamic parameters ΔH , ΔS and ΔG (Equations 9 and 10) presented in Table 5 were obtained from Figure 9. The negative ΔH indicates that the process is exothermic, confirming the adsorption theory for copper adsorption on calcined VL clay. The magnitude of the enthalpy variation achieved (+24.8 kJ.mol⁻¹) for copper adsorption on calcined Bofe clay showed that it is an endothermic processes.

A decrease in entropy during adsorption helps the stabilization of the metal-clay complex formed ($\Delta S < 0$). ΔS values suggest a decrease in randomness at the solid/solution interface during copper sorption on calcined VL

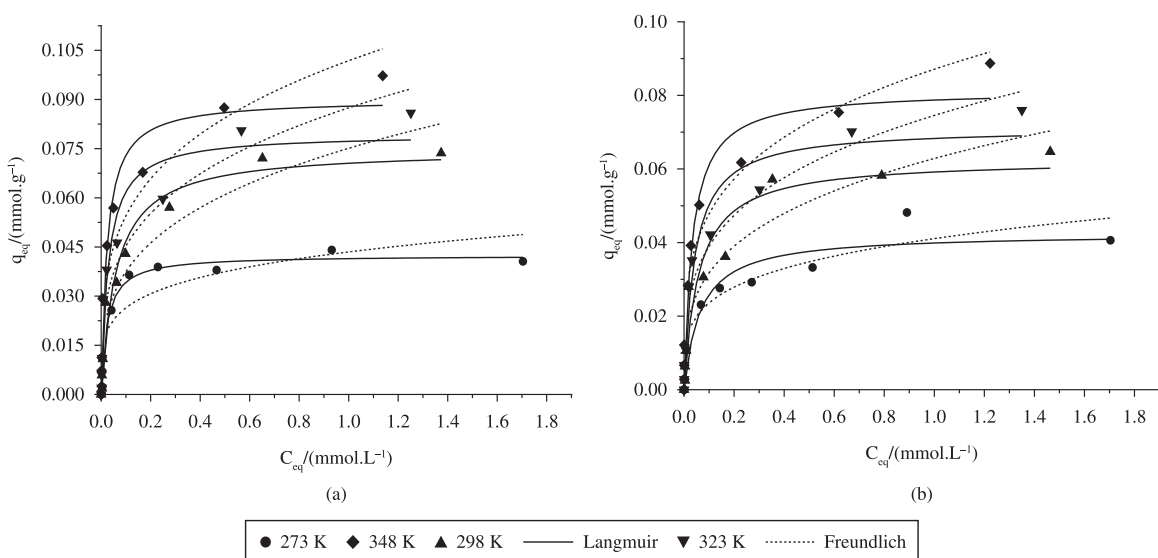


Figure 8. Adsorption isotherms for copper removal on: a) calcined Bofe clay, and b) calcined VL clay in different temperatures.

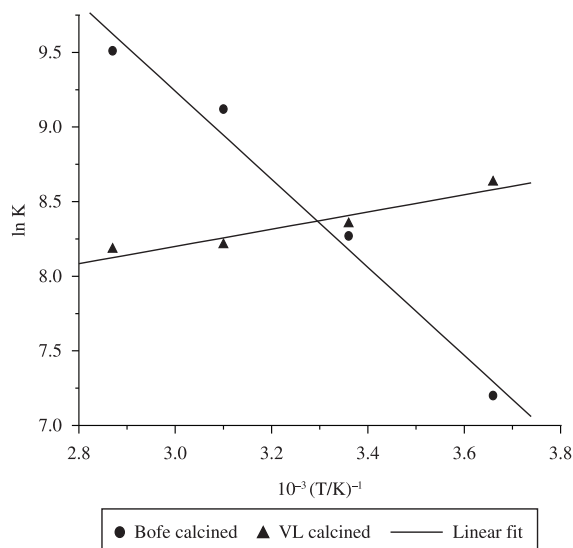
Table 5. Thermodynamic parameters of adsorption.

| System | ΔH (kJ.mol ⁻¹) | ΔS (J.(mol.K) ⁻¹) | ΔG (kJ.mol ⁻¹) | | | |
|------------------|---------------------------------------|--|------------------------------------|-------------------|-------|-------|
| | | | 273 K | T _{room} | 323 K | 348 K |
| Cu/calcined Bofe | +24.8 | +151.5 | -16.6 | -20.3 | -24.1 | -27.9 |
| Cu/calcined VL | -4.81 | +53.7 | -19.5 | -20.8 | -22.2 | -23.5 |

T_{room}: 298 K for Cu/calcined Bofe and 297 K Cu/calcined VL clays.

Table 6. Thermodynamic parameters data for Cu(II) in different clays.

| Clay | ΔH (kJ.mol ⁻¹) | ΔS (J(mol.K) ⁻¹) | Reference |
|--------------------------------|------------------------------------|--------------------------------------|--------------|
| Acid activated montmorillonite | +45.7 | +334.5 | 23 |
| Bentonite Turkey | +10.36 | +42.0 | 24 |
| Montmorillonite (M1) | +50.7 | +180.7 | 25 |
| Spent activated clay | +14.52 | +138.9 | 26 |
| Na-montmorillonite | +18.36 | -200.5 | 27 |
| NaDS-montmorillonite | +7.1 | +9.1 | 28 |
| Calcined Bofe | +24.8 | +86.4 | Present work |

**Figure 9.** Adsorbate distribution coefficient as function of temperature.

clay compared with Bofe clay. The clays–Cu interactions occurred spontaneously and were accompanied by a decrease in Gibbs free energy ($\Delta G < 0$). The degree of spontaneity was found to decline as the process temperature rose, ranging from -16.6 to -27.9 kJ.mol⁻¹ for the temperature range between 273 and 348 K. Adsorption and ion exchange of Cu(II) on different clays had already been reported as endothermic²³⁻²⁸, as shown in Table 6. It was likely that adsorption of Cu(II) ions on clay surface require an activation energy and rise in temperature helped more Cu(II) ions to overcome this energy barrier and get attached to the surface²³.

References

- Ghorbel-Abid I, Galai K and Trabelsi-Ayadi M. Retention of chromium (III) and cadmium (II) from aqueous solution by illitic clay as a low-cost adsorbent. *Desalination*. 2010; 256:190-195. <http://dx.doi.org/10.1016/j.desal.2009.06.079>
- Praus P, Turicová M and Valášková M. Study of silver adsorption on montmorillonite. *Journal of the Brazilian Chemical Society*. 2008; 19:549-556. <http://dx.doi.org/10.1590/S0103-50532008000300025>
- Sajidu SMI, Persson I, Masamba WRL and Henry EMT. Mechanisms of heavy metal sorption on alkaline clays from Tundulu in Malawi as determined by EXAFS. *Journal of Hazardous Materials*. 2008; 158:401-409. PMID:18329799. <http://dx.doi.org/10.1016/j.jhazmat.2008.01.087>
- Novakovic T, Rozic L, Petrovic S and Rosic A. Synthesis and characterization of acid-activated Serbian smectite clays obtained by statistically designed experiments. *Chemical*

4. Conclusions

The chemical composition of clays was not modified by calcination, but the Cation Exchange Capacity (CEC) was reduced. Adsorption results indicated that the sorption kinetics of copper ions by clays is rapid, requiring a minimum 60 minutes to reach equilibrium. The study of mass transfer parameters, as well as the breakthrough curves showed that the better appropriate operating outflow rate values, i.e. which minimizes the diffusional resistances in the bed for removal of copper by Bofe and VL calcined clays were of 4 and 3 mL/min, respectively. The breakthrough curves demonstrated that increasing the outflow rate, the breaking point, the point of saturation throughput and total removal values tend to decrease. The Langmuir isotherm model correctly represents the equilibrium data obtained from experiments in bath and in fixed bed at room temperature. At low concentrations, the removal of copper has a linear equilibrium and it does not depend on the system applied (static or dynamic). Calcination produced hydroxyl loss, preventing chemical precipitation of copper by alkalinity. The adsorption capacity (qm) increased in fixed bed, which suggests that copper adsorption on calcined Bofe and VL clays is related to the mobility of the particles. Copper adsorption on calcined VL clay is exothermic whereas on Bofe clay is endothermic. The clay-Cu interactions occurred spontaneously, being followed by a decrease in Gibbs free energy.

Acknowledgements

The authors acknowledge and thank the financial support received from CNPq and Foundation for Research Support of Sao Paulo State, FAPESP, for this research.

- Engineering Journal*. 2008; 137:436-442. <http://dx.doi.org/10.1016/j.ccej.2007.06.003>
5. Kubilay S, Gürkan R, Savran A and Sahan T. Removal of Cu(II), Zn(II) and Co(II) ions from aqueous solutions by adsorption onto natural bentonite. *Adsorption*. 2007; 13:41-51. <http://dx.doi.org/10.1007/s10450-007-9003-y>
 6. Stathi P, Litina K, Gournis D, Giannopoulos TS and Deligiannakis Y. Physicochemical study of novel organoclays as heavy metal ion adsorbents for environmental remediation. *Journal of Colloid and Interface Science*. 2007; 316:298-309. PMID:17804008. <http://dx.doi.org/10.1016/j.jcis.2007.07.078>
 7. Ouhadi VR, Yong RN and Sedighi M. Desorption response and degradation of buffering capability of bentonite, subjected to heavy metal contaminants. *Engineering Geology*. 2006; 85:102-110. <http://dx.doi.org/10.1016/j.enggeo.2005.09.031>
 8. Brigatti MF, Colonna S, Malferrari D, Medici L and Poppi L. Mercury adsorption by montmorillonite and vermiculite: a combined XRD, TG-MS, and EXAFS study. *Applied Clay Science*. 2005; 28:1-8. <http://dx.doi.org/10.1016/j.clay.2004.03.006>
 9. Bailey SE, Olin TJ, Bricka M and Adrian D. A review of potentially low-cost sorbents for heavy metals. *Water Research*. 1999; 33(11):2469-2479.
 10. Chen WJ, Hsiao LC and Chen KKY. Metal desorption from copper(II)/nickel(II)-spiked kaolin as a soil component using plant-derived saponin biosurfactant. *Process Biochemistry*. 2008; 43:488-498. <http://dx.doi.org/10.1016/j.procbio.2007.11.017>
 11. Kleinübing SJ, Vieira RS, Beppu MM, Guibal E and Silva MGC. Characterization and evaluation of copper and nickel biosorption on acidic algae *Sargassum Filipendula*. *Materials Research*. 2010; 13:541-550. <http://dx.doi.org/10.1590/S1516-14392010000400018>
 12. Meneghetti E, Baroni P, Vieira RS, Silva MGC and Beppu MM. Dynamic adsorption of chromium ions onto natural and crosslinked chitosan membranes for wastewater treatment. *Materials Research*. 2010; 13:89-94. <http://dx.doi.org/10.1590/S1516-14392010000100018>
 13. Vieira MGA, Almeida Neto AF, Gimenes ML and Silva MGC. Removal of nickel on Bofe bentonite calcined clay in porous bed. *Journal of Hazardous Materials*. 2010; 176:109-118. PMID:20022694. <http://dx.doi.org/10.1016/j.jhazmat.2009.10.128>
 14. Vieira MGA, Almeida Neto AF, Gimenes ML and Silva MGC. Sorption kinetics and equilibrium for the removal of nickel ions from aqueous phase on calcined Bofe bentonite clay. *Journal of Hazardous Materials*. 2010; 177:362-371. PMID:20042281. <http://dx.doi.org/10.1016/j.jhazmat.2009.12.040>
 15. Puigdomenech I. *Hydra and Medusa Programs*. Sweden: Royal Institute of Technology; 2004.
 16. Davranche M, Lacour S, Bordas F and Bollinger JC. An Easy Determination of the Surface Chemical Properties of Simple and Natural Solids. *Journal of Chemical Education*. 2003; 80:76-78. <http://dx.doi.org/10.1021/ed080p76>
 17. Langmuir I. The adsorption of gases on plane surfaces of glass, mica and platinum. *Journal of the American Chemical Society*. 1918; 40:1361-1403. <http://dx.doi.org/10.1021/ja02242a004>
 18. Freundlich HMF. Über die adsorption in lasugen. *Zeitschrift für Physikalische Chemie (Leipzig)*. 1906; 57A:385-470.
 19. Volesky B, Weber J and Park JM. Continuous-flow metal biosorption in a regenerable *Sargassum* column. *Water Research*. 2003; 37:297-306. [http://dx.doi.org/10.1016/S0043-1354\(02\)00282-8](http://dx.doi.org/10.1016/S0043-1354(02)00282-8)
 20. Santos PS. *Ciência e tecnologia de argilas*. São Paulo: Edgard Blücher Ltda; 1992.
 21. Zeta-Meter Inc. *Zeta-Potential: A Complete Course in 5 Minutes*. Staunton: Zeta-Meter, Inc.; 1997.
 22. Treybal RE. *Mass Transfer Operations*. New York: McGraw Hill; 1980.
 23. Bhattacharyya KG and Gupta SS. Removal of Cu(II) by natural and acid-activated clays: An insight of adsorption isotherm, kinetic and thermodynamics. *Desalination*. 2011; 272:66-75. <http://dx.doi.org/10.1016/j.desal.2011.01.001>
 24. Eren E and Asfin B. An investigation of Cu(II) adsorption by raw and acid-activated bentonite: A combined potentiometric, thermodynamic, XRD, IR, DTA study. *Journal of Hazardous Materials*. 2008; 151:682-691. PMID:17644249. <http://dx.doi.org/10.1016/j.jhazmat.2007.06.040>
 25. Bhattacharyya KG and Gupta SS. Adsorptive accumulation of Cd(II), Co(II), Cu(II), Pb(II), and Ni(II) from water on montmorillonite: Influence of acid activation. *Journal of Colloid and Interface Science*. 2007; 310:411-424. PMID:17368467. <http://dx.doi.org/10.1016/j.jcis.2007.01.080>
 26. Weng C-H, Tsai C-Z, Chu S-H and Sharma YC. Adsorption characteristics of copper(II) onto spent activated clay. *Separation and Purification Technology*. 2007; 54:187-197. <http://dx.doi.org/10.1016/j.seppur.2006.09.009>
 27. Lin S-H and Juang R-S. Heavy metal removal from water by sorption using surfactant-modified montmorillonite. *Journal of Hazardous Materials*. 2002; 92:315-326. [http://dx.doi.org/10.1016/S0304-3894\(02\)00026-2](http://dx.doi.org/10.1016/S0304-3894(02)00026-2)
 28. El-Batouti M, Sadek OM and Assaad FF. Kinetics and thermodynamics studies of copper exchange on Na-montmorillonite clay mineral. *Journal of Colloid and Interface Science*. 2003; 259:223-227. [http://dx.doi.org/10.1016/S0021-9797\(02\)00173-X](http://dx.doi.org/10.1016/S0021-9797(02)00173-X)

Appendix 1. Abbreviations.

| | |
|---|--|
| A | specific surface area (g.m^{-2}) |
| b, q_m | are Langmuir coefficients representing the equilibrium constant for the adsorbate–adsorbent equilibrium and the maximum adsorbed amount on the monolayer |
| C_0 | initial concentration of the metal in the liquid phase (mmol.L^{-1}) |
| C_a, C_b | concentration of acid and base added, respectively (mol.L^{-1}) |
| C_{eq} (mmol.L^{-1}) and q_{eq} (mmol.g^{-1}) | concentration of metal ions in the liquid and solid phases, respectively |
| C_i, C_f | the initial and final concentration of metal ion, respectively (mmol.L^{-1}) |
| C_m | represent the solid content (g.L^{-1}) |
| C_{Na}^+ | ion concentration Na^+ measured by atomic adsorption (mg.L^{-1}) |
| V_{NH4+} | volume of ammonium acetate 3M (mL) |
| f | conversion factor of sodium to equivalents |
| F | Faradays constant ($96,485.3399 \text{ Coulomb mol}^{-1}$) |
| K_d | adsorbate distribution coefficient (q_{eq}/C_{eq} em L.g^{-1}) |
| K_f, n | Freundlich coefficients |
| m | mass of adsorbent (g) |
| q | the adsorbed mass of metal ion per gram of adsorbent (mmol.g^{-1}) |
| R | universal gas constant ($8.314 \times 10^{-3} \text{ kJ (K.mol}^{-1})$) |
| T | temperature (K) |
| V | volume of solution (L) |
